ISBN: 978-3-95450-191-5 doi:10.18429/JACoW-SRF2017-TUPB082

SETUP OF A SPATIALLY RESOLVING VECTOR MAGNETOMETRY SYSTEM FOR THE INVESTIGATION OF FLUX TRAPPING IN SUPERCONDUCTING CAVITIES

B. Schmitz*, K. Alomari, J. Köszegi, O. Kugeler, Y. Tamashevich, J. Knobloch
Helmholtz-Zentrum Berlin, Germany

Abstract

Flux trapping is the major contribution to the residual resistance of superconducting cavities. In order to gain a better understanding of the mechanisms involved and aiming at an eventual minimization of trapped flux, a measurement setup based on AMR sensors was devised that allows for monitoring the magnetic field vector at various positions near the cavity surface. First results of the efforts are presented.

INTRODUCTION

The precise investigation of loss mechanisms in SRF cavities is the key to a comprehensive understanding of their limitations in both the quality factor and the accelerating gradient. To minimise these mechanisms it became evident [1], that the trapped magnetic flux needs to be examined more closely.

This has been done by placing fluxgate magnetometers in the cryostat [2] or next to the cavity [3] or even inside the cavity [4] and measuring the magnetic field before, during and after the phase transition directly. However, fluxgate measurements inhibit certain disadvantages: They are limited to one dimension, they average the field over a typical length of 20 mm, and they are quite costly with >1k€ per sensor. The usage of AMR sensors is a more favourable alternative at ~ 1€/sensor, as the usability has been demonstrated [5].

A magnetic mapping system was designed using many of these AMR sensors which allows a spatial vectorial measurement around the whole cavity. The general set up and the first results of the commissioning run are presented.

EXPERIMENTAL SETUP

For the mapping of the magnetic field around a cavity, arrays of AMRs have been created. These arrays are distributed on different PCB boards to allow a variable and flexible placement around a cavity or any other sample that needs to be evaluated. At each position 3 sensors are installed, one for each spatial direction.

The connection toward the outside of the cryostat is done via 41 pin military vacuum feed-throughs. For data acquisition an imc spartan device without any additional operational amplifiers or analogue to digital converters was used. imc spartan itself provides an analogue to digital converter as well as an amplifier for each of its 128 channels. We were able to measure voltage drops in the region of few µV which corresponds to a few µT. The control of the whole setup was done by an integrated LabView routine.

* benedikt.schmitz@helmholtz-berlin.de

The arrays were placed around a cavity during a vertical test as depicted in Fig. 1.

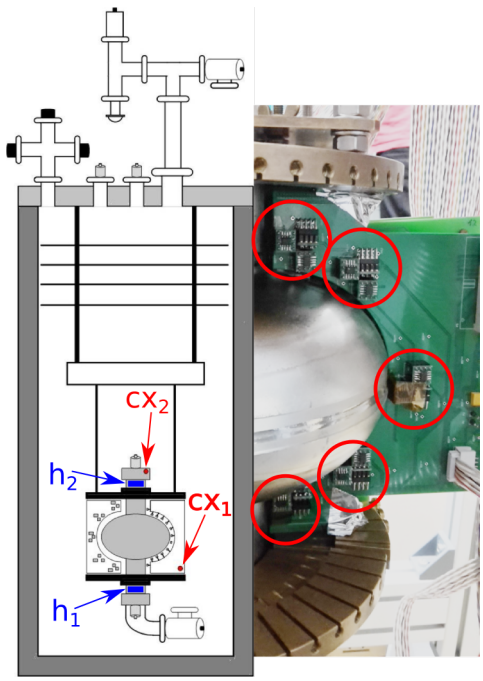

Figure 1: The left side shows an overall view including the position of two cernox sensors (red dots). *Cernox 1* (short: cx_1) measured the Helium bath temperature at the lower edge of one magnetic board. *Cernox 2* (short: cx_2) measured the temperature at the top flange of the cavity's beam pipe. The blue positions show where the two heaters of the cavity are fixed. Heater 1 (short: h_1) on the lower beam pipe and Heater 2 (short: h_2) on the upper beam pipe. The magnetic mapping has also been coupled with a thermometry system, which can be seen on the right side of the setup sketch. The right side shows a picture of the setup. The magnetic boards are fixed around the cavity, so that the sensors get as close as possible to the cavity surface. Each red circle includes one three dimensional measurement point.

Setup of Array

The whole setup consists of a specific number of PCB boards. Here we used four boards arranged around the cavity in 90° steps. Each PCB has a shape similar to boards used in thermometry [6] that allows to place sensors on the cavity surface. All boards are attached to the cavity with a holder, every board had its own feedthrough, so that it is possible

ISBN: 978-3-95450-191-5 doi:10.18429/JACoW-SRF2017-TUPB082

to piece different boards together arbitrarily, based on the scientific questions. Each board has the following features:

- 5 Groups with 3 AMR sensors each. Each group measures the field projection in $\vec{e}_r$, $\vec{e}_\varphi$ and $\vec{e}_z$.
- Low-pass and capacitors allow filtering of noise and peaks on the supply voltage line. This is done to ensure that stray fields are damped.
- Empty pins on the board allow for the integration of additional sensors or devices for specific measurements (e.g., fluxgate magnetometers, cernox sensors, coils).
- Integrated test coils allow for calibration at arbitrary conditions.

With the projection measurement in $\vec{e}_\varphi$ it is also possible to determine fields that are induced by thermocurrents.

AMR Sensors

AMR stands for "Anisotropic MagnetoResistivity". The resistance of such a material changes with the magnetic field. For low fields (lower than 200 µT, one can construct a linear sensor which produces an output voltage which is directly proportional to the applied field. To increase the sensitivity a Wheatstone bridge has been used. The sensitivity at room temperature is in the order of 12 mV mT^{-1}/V. Because of the high shift in resistance due to temperature change, the sensitivity highly increases (factor of 3 for liquid nitrogen). Therefore it was possible to measure fields down to a few µT.

MEASUREMENT

The system was installed on a DESY single cell cavity and underwent a vertical test. Data was recorded constantly at 20 Hz starting at the initial cool down until the final warm up. The AMR sensors were able to reproduce the signatures of the phase transition, which are known through previous measurements with fluxgate magnetometers [7].

Phase Transition Measurement

The setup has been tested for the first time. For these results the known properties of the phase transition for the niobium cavity have been used. One measurement example can be found in Fig. 2. This transition was measured during the warm-up for a thermal cycling of the cavity.

First thing to note: The absolute value of field, measured at one sensor, changes. The measured field in $\vec{e}_\varphi$ direction did not change significantly. For the other two directions a significant change is visible. During the shown measurement, a heater – attached to the bottom of the cavity – was used. Since no cernox was attached near to this position, one can not easily reconstruct the resulting temperature gradient along the cavity surface.

Each temperature cycling causes two phase transitions – one during warm up when the cavity changes from superconducting to normal conducting state and one during cool down when the cavity changes from normal conducting to superconducting state. The shown signature in Fig. 2 was reproducible during the whole measurement run.

Further on we see, that the critical temperature is reached by the temperature sensors approximately 3 minutes after the phase transition was measured by the magnetic sensors. The main reason for this discrepancy is the deviating position of the different sensors. Currently it is not possible to determine the temperature value directly at the magnetic sensors. This is subject of change for the next iteration of the whole setup.

Velocity of Transition

To demonstrate the spatial resolution and the time resolution one additional evaluation is done.

If the peaks, shown in Fig. 2, are used as an indicator for a phase transition from superconducting to normal conducting phase, then it is possible to determine a velocity of the phase front, while it travels through the cavity.

In Fig. 3 the position in z direction is plotted versus the time when the transition is detected at a specific sensor.

Due to this resolution a possibility arises to determine the velocity of the transition travelling through the cavity

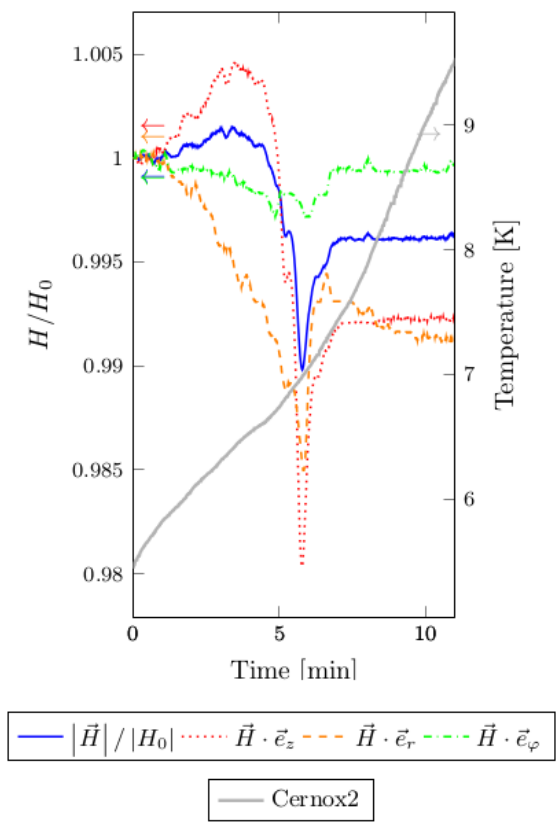

Figure 2: The left axis indicates the measured field normalized to the constant field value at the time $t = 0$ min. The right axis denotes the temperature measured with the cernox sensors. Only the results of *Cernox 2* are plotted. cx_2 measured the temperature at the top flange of the cavity's beam pipe. Its position is shown in Fig. 1 as red dots.

ISBN: 978-3-95450-191-5 doi:10.18429/JACoW-SRF2017-TUPB082

along the z-axis. Since the signals are noisy the extracted times of the transitions at each sensor exhibits a fairly large error bar as indicated in Fig. 3. From the times and the positions of the sensors, the phase front velocity has been calculated. Because of the used, asymmetrically fixed, heater different influences on the lowest sensors are seen. This inhomogeneity causes a shift of the first registered transition which can be seen in Fig. 3. The closer the magnetic sensor is to the heater, the earlier it shows a phase transition. The sensor that is farthest away from the heater is less influenced by it. Because of this, the first two data points on the left side are systematically shifted to the left – and register the phase transition earlier – and are therefore neglected in the calculation for the phase transitions velocity. Therefore the systematic uncertainty of the final velocity is reduced.

To determine the velocity of the phase front all points that are not influenced are taken into account and a linear regression has been done. Linear dependency was assumed to be a first order approximation and sufficient for the current resolution of the array.

The velocity is given via the slope of the regression curve, so that we can assume for this specific situation, that $v = 2.9(3)\,\mathrm{mm\,s^{-1}}$.

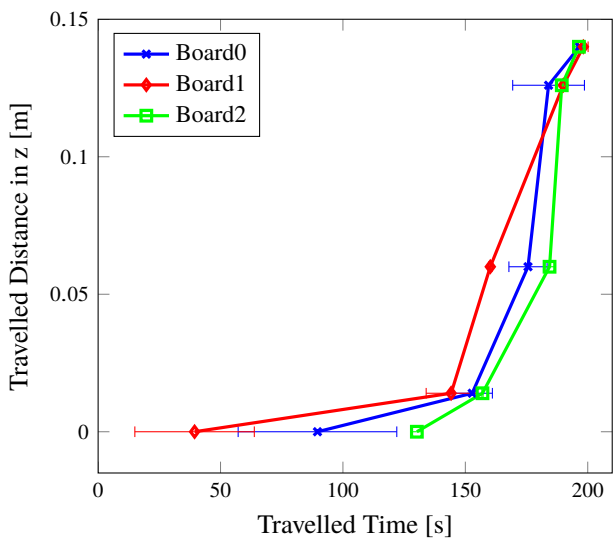

Figure 3: This figure depicts the path of the superconducting phase through the cavity. It is displayed for 3 different PCB boards. This measurement was done during a warming up above the critical temperature that was done with a heater connected to the lower beam pipe of the cavity. Every point is displayed with the $1-\sigma$ uncertainty.

CONCLUSION AND OUTLOOK

The array and the magnetic sensor have been successfully tested. AMR sensors have shown to be an efficient alternative to fluxgate magnetometers, allowing for easy rescaling of the experiment to satisfy arbitrary measurement conditions.

Optimization of the setup are still ongoing, such that a sensitivity of nT will be possible in the near future. Further more, the use of more dense packs of sensors will also allow to get a better resolution of magnetic field around the cavity. Since AMR is only one effect of the family of xMR effects, even better sensor concepts are being evaluated for the usage and handiness in SRF research.

Concerning the velocity of the phase front: A first approximation has been done. The main influence on this velocity is the thermodynamic process of warming up.

REFERENCES

[1] O. Kugeler, J. Vogt, J. Knobloch, and S. Aull, "Impact of Trapped Flux and Thermal Gradients on the SRF Cavity Quality Factor", in *Proc. IPAC'12*, New Orleans, LA, USA, May 2012, p. 2203.

[2] S. Aull *et al.* "Trapped magnetic flux in superconducting niobium samples", Physical Review Special Topics - Accelerators and Beams. (2012); 15:1-6.

[3] A. Romanenko *et al.* , "Ultra-high quality factors in superconducting niobium cavities in ambient magnetic fields up to 190 mG", *Applied Physics Letters*, 105, 234103 , 2014, arXiv:14107877. (2014)

[4] J. Köszegi, "Surface Resistance Minimization in SRF Cavities by Reduction of Thermocurrents and Trapped Flux", Dissertation, to be published in (2017), Universität Siegen

[5] A. Becker, to be published in (2017), Universität Siegen

[6] J. Knobloch *et al.*, "Design of a high speed, high resolution thermometry system for 1.5 GHz superconducting radio frequency cavities", *Review of Scientific Instruments* 65, 3521 (1994); http://dx.doi.org/10.1063/1.1144532

[7] S. Posen *et al.*, "Efficent expulson of magnetic flux in superconducting radiofrequency cavities for high Q_0 applications", Journal of Applied Physics 119, 213903 (2016), doi: 10.1063/1.4953087 http://dx.doi.org/10.1063/1.4953087